IAC-23-D3.2B.x78354

In-Orbit Assembly: A Baseline for Large Space Structures through Standardised Tiles and Interfaceable Elements

Yi Qiang Ji Zhang[a]*, Rachel Wright[b], Sara Alao[c], Triyan Pal Arora[d], James Nathan Fernandes[e], Roman Haskett[f], Xabier Idiondo[g], Adrien Kreutz[h], Pablo Javier Rodriguez Gomez[i], Maria Martinez Galisteo[j], Óscar Santín[k], Yacine Soltani[l], Leonard Felicetti[m], Saurabh Upadhyay[n]

[a] *School of Aerospace, Transport and Manufacturing, Cranfield University, College Rd, Wharley End, Bedford, United Kingdom MK43 0AL,* yiqiangjizhang@gmail.com
[b] *School of Aerospace, Transport and Manufacturing, Cranfield University, College Rd, Wharley End, Bedford, United Kingdom MK43 0AL,* rachel.wright.046@cranfield.ac.uk
[c] *School of Aerospace, Transport and Manufacturing, Cranfield University, College Rd, Wharley End, Bedford, United Kingdom MK43 0AL,* sjalao16@gmail.com
[d] *School of Aerospace, Transport and Manufacturing, Cranfield University, College Rd, Wharley End, Bedford, United Kingdom MK43 0AL,* triyanpal.arora.225@cranfield.ac.uk
[e] *School of Aerospace, Transport and Manufacturing, Cranfield University, College Rd, Wharley End, Bedford, United Kingdom MK43 0AL,* nathan.fernandes.880@cranfield.ac.uk
[f] *School of Aerospace, Transport and Manufacturing, Cranfield University, College Rd, Wharley End, Bedford, United Kingdom MK43 0AL,* roman.haskett.652@cranfield.ac.uk
[g] *School of Aerospace, Transport and Manufacturing, Cranfield University, College Rd, Wharley End, Bedford, United Kingdom MK43 0AL,* xabier.idiondogoni.132@cranfield.ac.uk
[h] *School of Aerospace, Transport and Manufacturing, Cranfield University, College Rd, Wharley End, Bedford, United Kingdom MK43 0AL,* adrien.kreutz.458@cranfield.ac.uk
[i] *School of Aerospace, Transport and Manufacturing, Cranfield University, College Rd, Wharley End, Bedford, United Kingdom MK43 0AL,* Pablo.Rodriguez@cranfield.ac.uk
[j] *School of Aerospace, Transport and Manufacturing, Cranfield University, College Rd, Wharley End, Bedford, United Kingdom MK43 0AL,* mariamartinezgalisteo@gmail.com
[k] *School of Aerospace, Transport and Manufacturing, Cranfield University, College Rd, Wharley End, Bedford, United Kingdom MK43 0AL,* oscar.santinblanco.742@cranfield.ac.uk
[l] *School of Aerospace, Transport and Manufacturing, Cranfield University, College Rd, Wharley End, Bedford, United Kingdom MK43 0AL,* yacine.soltani.807@cranfield.ac.uk
[m] *School of Aerospace, Transport and Manufacturing, Cranfield University, College Rd, Wharley End, Bedford, United Kingdom MK43 0AL,* leonard.felicetti@cranfield.ac.uk
[n] *School of Aerospace, Transport and Manufacturing, Cranfield University, College Rd, Wharley End, Bedford, United Kingdom MK43 0AL,* saurabh.upadhyay@cranfield.ac.uk
* Corresponding Author

Abstract

Novel mission concepts require larger space structures. Concepts such as space-based solar power, large scale communications systems, in-orbit manufacturing, are not possible to be achieved without in-situ assembly due to launch vehicle constraints.

This paper details a description of an in-orbit assembly mission utilising robotic assemblers. The aim of the mission is to test novel technologies to be used in space assembly. Specifically, we propose to use a standardised and modular tile that can embed diverse types of payloads, provide locomotion, and act as a structural element by creating a more robust and sounder base frame. The expected benefits of this multifunctional tile are: reduction of production costs, ease of the in-orbit assembly process and a high degree of storage inside the cargo spacecraft.
The current mission profile considers the launch of two spacecraft: a Hub station with the power and AOCS subsystems to support the assembly and maintain operative the large structure and a Supply Vehicle with cargo storage capability for the tile components.

A 6 degree of freedom robotic arm will navigate through an electrically powered rail system embedded on the backside of the tile structure, performing the assembly process. The tiles would be picked by the arm and transported from the

cargo vehicle to the assembly place, interlocked with other tiles through an interface, building up the size of the structure and the reach of the Assembler. The payload interface at the frontside of the tile is designed to accept various kinds of applications that can be replaceable. The Hub provides AOCS, power, and communications to the structure during assembly.

The baseline design presented in this paper is intended to be used as a starting point and reference source for future developments regarding in-orbit assembly. This solution allows for a more streamlined and efficient approach to space assembly, compared to other emerging mission concepts for in-orbit assembly. Additionally, it enables the repurposability of the structure for multiple applications throughout the mission's timeline. The feasibility of the mission concept is demonstrated throughout the assessment of the imposed mission requirements and the estimation of mass and cost budgets. The scalability model created by this concept enables the definition of ambitious projects and applications of large space structures for years to come.

Keywords: In-orbit assembly, Space robotics, Large space structures, In-situ assembly, Mission design

Acronyms/Abbreviations
Attitude and Orbit Control Subsystem (AOCS)
Autonomy Requirements Engineering (ARE)
Computer-Aided Design (CAD)
Concurrent Engineering (CE)
Degrees of Freedom (DOF)
European Cooperation for Space Standardisation (ECSS)
End Of Life (EOL)
Group Design Project (GDP)
Geostationary Orbit (GEO)
Guidance, Navigation and Control (GNC)
Graveyard Orbit (GYO)
James Webb Space Telescope (JWST)
Low Earth Orbit (LEO)
Local Time of the Ascending Node (LTAN)
Multiple Arm-Robots for In-Orbit Operations (MARIO^2)
Medium Earth Orbit (LEO)
Model-Based Systems Engineering (MBSE)
On-Board Data Handling (OBDH)
Preliminary Design Review (PDR)
Space-Based Solar Power (SBSP)
Sun Synchronous Orbit (SSO)
Supply Vehicle (SV)
Technology Readiness Level (TRL)

1. Introduction

The need for large structures in space applications has increased in the last decade. The basis for this trend is due to the exigencies of new mission concepts which require the assembly of large infrastructures enabling enhanced performance or new applications. Large space structures are indeed seen as necessary for new optical space telescopes, if the required resolution and sensitivity needs to go beyond James Webb's one [1, 2]. On the other hand, space-based Solar Power needs kilometric mirrors or solar panels to be deployed in space to collect solar radiation. In the context of the increased exploitation of space for the new space economy, large telecommunication antennas are considered a beneficial asset which could increase the performance and the coverage of already existing and future services, providing a bigger economic return on the investments.

Analogously, the same trend has been observed in other fields such as robotics for assembly space infrastructures. Given the challenging conditions of deep space that pose on humans, robotic assemblers serve as viable alternatives for executing tasks in this environment because they can perform all those tasks without risking any human life.

For instance, it took nearly six months for the James Webb telescope to fully deploy its instruments and begin scientific operations [3]. This is because one of the key challenges that all space missions are facing is the reverse engineering necessary to design a payload capable not only of withstanding the stresses of rockets at launch but also meet the size and volume constraints imposed by the launcher's fairing. The cost needed to develop and launch a large structure using a single launch into orbit can be prohibitively expensive and is not feasible with current launcher capabilities. In contrast, parts of the structure can be more affordably brought in space by more launchers and assembled in orbit. Flexibility in design is a key benefit of in-orbit assembly and directly the question of why in-orbit assembly is needed.

Two of the biggest challenges in designing and deploying such a system are the destabilising torque on the whole assembly and the risk of debris impact failures. Both factors affect the performance of missions and require mitigation strategies to overcome. The Attitude Control System as such is crucial for maintaining stability and providing the pointing accuracy required for a mission of this sort. With the increase in the size of the structure, the complication of controlling the structure also grows. The manoeuvrability of the structure lowers as more torques are required to move the structure, being able to compromise its mechanical integrity. In addition, a large structure can be exposed to larger environmental torques depending on the orbital altitude and the required orientation. It becomes essential to study the dynamics and the controllability of large space structures to provide

the specific solutions to achieve the desired pointing needed for the success of the mission.

Similarly, recent proposals for in-orbit assembly technology often have a high demand for power. The launch size constraints have an impact on the design of the power subsystem which needed to be addressed with a specific orbit selection and trade-offs. The multiple systems deployed for this type of mission as well as the orbit require a specific communication architecture and topology to enable autonomous operations, the robust transmission of data and match operation goals. Still, the technology for completely autonomous robots is under development and despite their potential applications in numerous operations such as servicing, docking, transporting, debris removal, and refuelling, among others; there are many technical challenges that must be studied. Further research is needed to validate their viability for enabling future and more novel technologies.

The space industry is aware of this necessity and robot solutions have been studied and designed, and even sent into space. The locomotion of the robots and the interfaces are key elements to consider when assembling a large structure because they allow the robot to move across the structure and manipulate the structural parts. Some concepts as "walking" with the robotic arms throughout the structure, Multi-arm Installation Robot for Readying ORUS and Reflectors (MIRROR) [4], or translating itself through single axis rails, as the European Robotic Arm (ERA), both by the European Space Agency (ESA) [5], have been an inspiration for the project. Literature shows there are a large number of publications describing space assembly [6] [7] [8] [9]. The assembly and locomotion strategies can be classified in three different categories, represented in Fig. 1. The self-assembly strategy uses robotic arms to build a structure around a central body: the size of the structure is limited by the maximum reach of the arm. Crawling concepts might extend the reach and therefore the size of the structure to be build, however the selection of the locomotion strategy might affect the orbital and attitude keeping of the overall system. Assembly concepts based on free flying assemblers might overcome these issues, but require fuel and complex operations to be performed in orbit. The solution presented in this paper intends to tackle the numerous challenges of in-orbit assembly by demonstrating a set of technologies required to build large space structures in orbit. We propose a novel mission concept for assembling structures in space with robotic assemblers. To do so, we propose using a squadron of single-armed robotic assemblers to perform the in-orbit operations. MARIO2 (Multi Arm-Robots for In-Orbit Operations). This innovative approach offers a promising avenue for efficient and precise assembly operations in a challenging zero-gravity environment. The concept is based on the utilisation of standard modular tiles that not only can be manipulated with ease

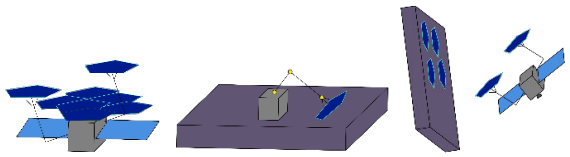

Fig. 1. Self-assembly assembler (left), crawler assembler (middle), free-flying assembler (right).

by the robots and distribute electrical power to the overall structure but also serve a dual role in providing locomotion for the assemblers to displace through while simultaneously ensuring structural integrity, thus enhancing the overall robustness of the assembly. Additional benefits of using these multifunctional tiles lay on the reduction of production costs, ease of the in-orbit assembly process and a high degree of storage inside of eventual cargo spacecraft.

This paper describes the baseline mission concept design based on the results of a four-month work of a team of students in Cranfield University. This exercise aimed to demonstrate the concept's feasibility by applying a systematic system engineering approach, assessing the overall design against requirements, and accurately analysing and evaluating the design budgets.

The structure of the paper reflects this strategy: Section 2 presents the mission's goal and objectives, followed by the top-level requirements and constraints used to scope and shape the design.

Subsequently, the baseline of the mission is explored in detail in Section 3. This includes the description of all 4 phases of the concept of operations, starting from the launch and early operations, the demonstration phase, operational phase and exploring end-of-life options with a primary focus on sustainability considerations.

Next, the payload (robotic Assembler and tiles), which is the main key innovation area in this paper is discussed in detail in Section 4. This section encompasses a detailed exposition of the design of the robotic manipulators, the locomotion algorithm, the design of the Hub and supply vehicle, along with a thermal, structural analysis and ending with the electrical power subsystem and communications. Next, Section 5 explores the ideal orbit, propulsion system and the attitude control of the vehicles. Section 6 details the mechanical and thermal subsystem. The electrical and communication subsystem are discussed in Section 7 and 8. Finally, Section 9 provides a breakdown of mass, power and cost budgets of every element.

2. Mission Definition

This section gives the background and motivation of the mission. It introduces aims and objectives as well as the top-level requirements and constraints shaping the overall mission concept.

2.1 Mission aim and objectives

The mission aims to design and demonstrate the necessary technology for in situ in-orbit assembly of large planar structures through robotic assemblers to support the next generation of space missions. Hence, increasing the TRL, bringing the technology closer to operational readiness, fostering advancements in space exploration capabilities by setting a base for future missions.

To fulfil the mission aim, two fundamental technological objectives have been identified:

- To demonstrate planar standardised and robotic elements for In-Orbit Assembly.
- To develop a reference source for sustainable future space developments.

2.2 Mission requirements and constraints

The mission was driven by the following Top-Level Requirements:

1. The mission shall be a technology demonstration mission for In-Orbit Assembly.
2. The In-Orbit assembly operation shall be conducted utilising one or more robotic assemblers.
3. The assemblers shall assemble a planar space structure from standardised modular units.
4. The assembled planar structure shall act as a baseline for future space applications, such as Space-Based Solar power, Large Scale Communications or Ultra-Wide Telescopes.

3. Mission Architecture and Concept of Operations

The baseline mission concept, obtained through the iteration of different solutions over a period of 4 months by a team of students at Cranfield University, is presented in this section. In addition, a tentative concept of operation is also presented under the assumption that the main mission aim is to demonstrate robotic assembly in orbit, but at the same time host possible payloads to be used in a second phase of the mission.

3.1 Mission architecture

The mission is composed of 4 essential elements. First, the overall mission concept is built around the utilisation of a standardised and *modular tile*, or building block for the structure, that can embed diverse types of payloads, provide locomotion, and act as a structural element by creating a more robust and sounder base frame. A representation of the modular tile is shown in Fig. 2. Such a structure embeds a surface that can host payloads such as solar panels, mirrors or phased array antenna systems. The tile also embeds a rail, which provides the double functionality of allowing locomotion

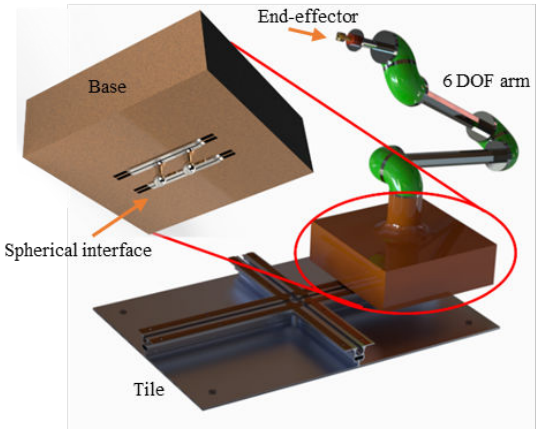

Fig. 2. Modular tile, assembler and locomotion system.

of eventual robotic platforms moving through it and providing structural integrity to the overall structural compound when built. Each of the 128 tiles used for the demonstration mission measures $1.5m \times 1m \times 0.11\ m$, with a mass of 21 kg.

The *Assembler* is the second main element of the mission. This key element is a specialised robot whose main tasks is to assemble/disassemble the tiles to build the final structure. As shown in Fig. 2, it possesses a 6-degree-of-freedom robotic arm, capable of handling loads of up to 50 kg. The overall dimensions of the robot are 60 cm x 60 cm x 20 cm and it weighs 53.2 kg. In terms of assembly philosophy, this robotic system navigates along the rails on the already placed tiles bringing each time one tile from the storage of a Supply Vehicle to the point where the tile needs to be assembled. A representation of the overall system is shown in Fig. 3 where the assembler is represented when returning to the

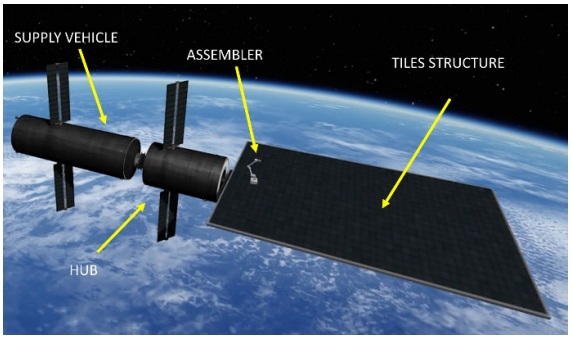

Fig. 3. Main components of the MARIO2 mission.

Hub after placing a tile on the edge of the flat structure.

The *Hub* provides the AOCS for the structure and also the power to the robots. Furthermore, it is the core unit where all the operations for the squadron of assemblers are computed and planned. The diameter of this vehicle is 4.2 m wide and a length of 6 m. Moreover, it possesses a dry mass of 5814 kg and a wet mass of 5966 kg. This Hub contains the subsystems required to maintain the

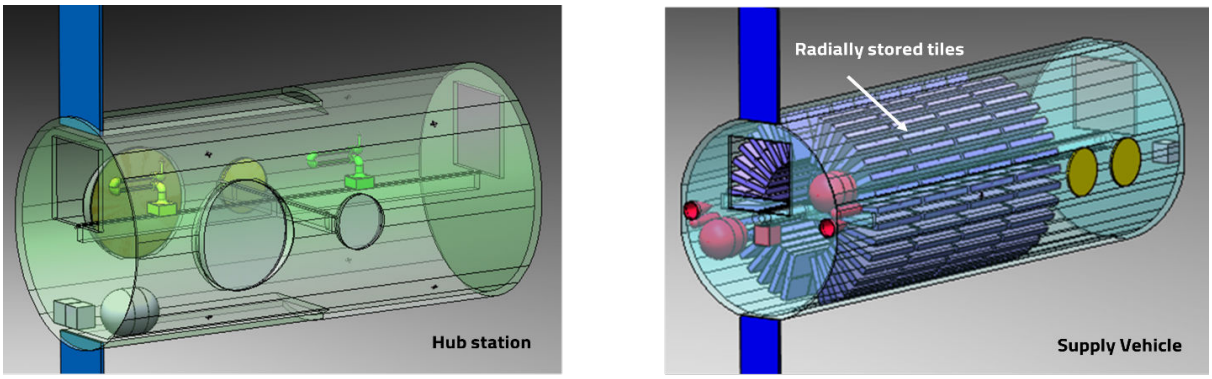

Fig. 4. The Hub (left) and the Supply Vehicle (right).

orbit and perform attitude and orbital manoeuvres. Additionally, the Hub will also supply electrical energy to both the robots and the payload above the tile. It is located on a side of the planar structure and will be the gateway between the Supply Vehicle (SV) and the assembled structure. Also, in terms of servicing, the Hub will be the place where assemblers perform servicing and maintenance operations on the payload and on tiles that have failed.

Parallel to the Hub, the SV shares the same diameter of 4.2 m. However, it extends to a length of 12 m. The SV exhibits a dry mass of 7648 kg and a wet mass of 12113 kg. It is a vehicle which will host all the payload and tiles in a radial form. This radial configuration was the result of several concepts on how to optimise space for the maximum amount of payload inside the vehicle. Preliminary configurations of the Hub and SV are illustrated in Fig. 4, alongside the internal disposition of the tiles inside the SC.

3.2 Concept of operations

The concept of operation is represented in Fig. 6. Two launches are planned considered for the demonstration mission: the Hub station will carry the robotic assemblers and all the necessary subsystems to guarantee power, communications and AOCS capabilities during the different phases of the assembly and operations of the structure; the SV will also be launched in order to bring the tiles necessary for the construction.

The mission timeline is split into a demonstration phase and an operational phase. The demonstration phase will encompass the full verification, testing and commissioning of all the technologies and required operations such as assembly and disassembly. The operational phase acts as a mission extension after the two years of validation, over the course of an extra 8 years, to continue the lifetime of the structure, as well as any further necessary data collection and to promote additional use of such a technology by third parties.

The orbit selected for the mission is a 3300 km altitude SSO in a dusk-dawn configuration. To place both Hub and SV in this orbit, two launches will take place from Vandenberg USA using both Falcon 9 for the Hub and Falcon Heavy for the Supply Vehicle. The exact time of launch is specified such that upon arrival to the operational orbit, the associated ascending and descending nodes align with 'Earth's terminator or in other terms, the LTAN is 06:00. It should be noted that the second launch, which concerns the SV, is scheduled to launch a day after the Hub is launched, providing that nominal health checks are achieved by the Hub once in the operational orbit.

For the demonstration of assembling the desired structure, the Supply vehicle will rendezvous and dock the Hub. Two assemblers will navigate with the aid of a path planning algorithm through an electrically powered rail system embedded on the backside of the tile structure, performing the assembly process. The locomotion will be aided by tracks and sphere joint interfaces to translate themselves through the rail system. The tiles will be grabbed by the arm, and then transported from the SV to the corresponding assembly position, and then interlocked with another tile through an interface. The Hub will provide attitude and orbit control, power, and communication between MARIO2 with Ground Stations as well as manage and monitor the performance of the Assemblers, during assembly.

At the EOL, the Hub and SV will dissipate all onboard energy sources and remain orbiting in a Graveyard orbit (GYO). The spacecraft and structure

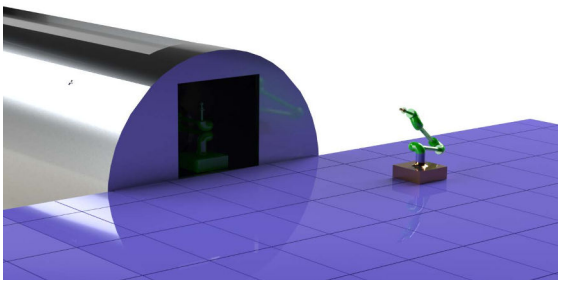

Fig. 5. Hub with assembler (left) and assembler (right).

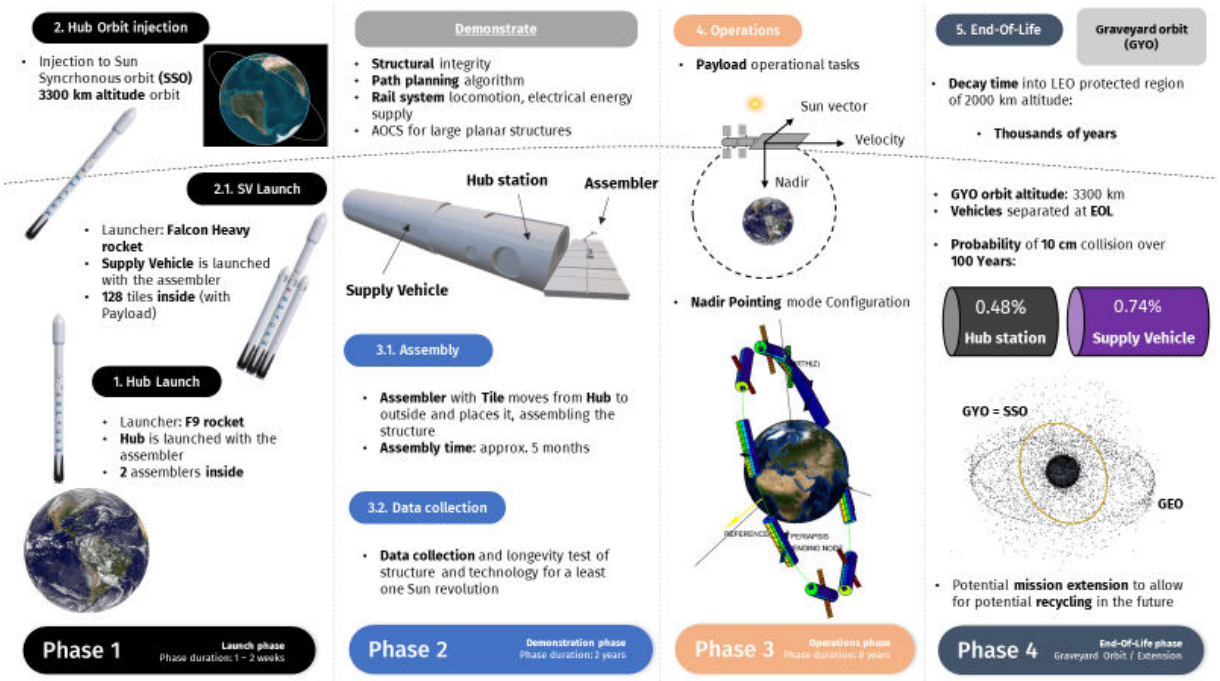

Fig. 6. MARIO2's concept of operations.

resources will be made available to be recycled or serviced once the mission is over.

4. Robotic Technologies

This section discusses the robotic assembler design followed by its assembly operations and autonomous path planning.

4.1 Design of the Robotic Assembler

The robotic assembler comprises three components: a base, an arm and an end-effector as shown in Fig. 2.

The *base* represents the pillar of the assembler and is firmly affixed to the rail. Within this base resides the locomotion mechanisms driven by motors and belts, an energy storage unit (battery), a central processing system, a braking system, and a compact antenna. These components collectively serve as the core infrastructure, facilitating the assembler's mobility, power supply, processing capabilities for autonomous operations, and communication functionalities.

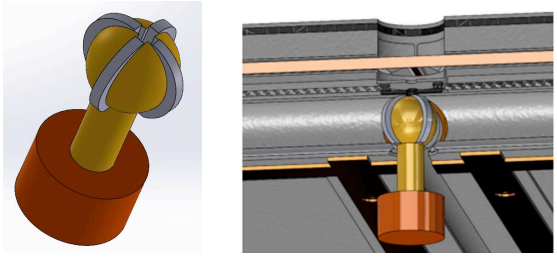

Fig. 7. Assembler's spherical end-effector with metal extrusions (left) and inside the tile (right).

The robotic arm is connected to the base on one end and the second end has an end-effector. The end-effector grabs and displaces tiles from one place to another. It is characterised by a spherical structure with four embedded metal extrusions that facilitates the attachment of the manipulator to the structural tile as shown in Fig. 7. However, it is essential to note that this attachment mechanism relies upon the presence of perforations within the central rail junction of the tile. These perforations function as secure anchor points to which the manipulator's end-effector can firmly latch.

4.2 Locomotion system

The free-flying system, inspired by MIT's SPHERES project, uses robots with thrusters and fuel tanks to move around the structure [10]. The crawling system, based on ESA's MIRROR project, employs robots with three arms for crawling and transporting tiles [11]. In contrast to the flying and crawling robots, the proposed robot uses rail locomotion on an integrated rail system within the modular tiles for assembler navigation.

The assemblers have guiding spheres and belts situated underneath the robot base as part of a 'skid locomotion system'. This enables the assemblers to move successfully through the matrix of standard tiles. The standardised tiles have rails attached to the underside of them, upon which the guide spheres and belts move along. Both the spheres and the tracks are in contact with the rails via friction which ensures assembler movement, as no gravity force is present. To maintain contact, two guiding spheres are connected by a linear actuator to the

Table 1. Locomotion systems trade-off table.

Trade-Off Parameters	Flexibility of Operations		Time Efficiency		Complexity of Control		Maximum Assembler Distance From Hub		System Design's Total Mass		Technology Readiness Level		Total
Weightings (Out of 6)	5		3		5		3		3		6		
Scoring	Score (Out of 5)	Total	Score (Out of 5)	Total	Score (Out of 5)	Total	Score (Out of 3)	Total	Score (Out of 10)	Total	Score (Out of 9)	Total	
Rail (attached)	4	20	3	9	5	25	3	9	6	18	7	42	123
Crawler (3 arms)	4	20	2	6	2	10	1	3	6	18	7	42	99
Free-flying + dock	5	25	3	9	1	5	2	6	5	15	8	48	108

base of each assembler. The linear actuator exerts a force to regulate the separation between the base and the rails, ensuring the contact between the tracks, the rails and the spheres. The skid locomotion has a motor to drive the belts which allows the assemblers to accelerate, reach a desired constant velocity, and then decelerate.

To justify the selection, a trade-off analysis was performed focusing on flexibility of operations and time efficiency. Flexibility of operations evaluates the variety of tasks the assemblers can perform, while time efficiency measures the speed of completing the assembly. The results of the trade-off analysis are presented in the Table 1.

Flexibility of operations analysis showed that the rails and crawling systems scored 4 out of 5 points, where they were restricted to the structure, while the free-flying system scored 5 out of 5, capable of operating in various environments. Time efficiency analysis used a MATLAB script, revealing that the rails system would take 13 days, scoring 3 out of 5, the free-flying system 26 days, also scoring 3 out of 5, and the crawling system 41 days, scoring 2 out of 5.

The trade-off table results favoured the rail locomotion system. Although less versatile than the free-flying system, its advantages in speed, precision, and control make it the optimal choice for the MARIO2 mission.

4.3 Robotic assembly operations

The 6 DOF robotic arm is tasked with executing a spectrum of actions essential for the assembly procedure. The robotic arm simulator (RAS) tool was used to simulate the operations and demonstrated that with only 6 DOF it was able to successfully execute all assembly tasks.

One of the major challenges for the robotic assembler is to compute the most efficient trajectory that its arm will need to follow to carry tiles and payload while considering various constraints such as disturbance torques, power consumption, energy usage, and collision avoidance. The following three operations are considered for the structure assembly process: operation 1 (OP1), operation 2 (OP2) and operation 3 (OP3).

In OP1, the robotic arm retrieves the tile from the cargo vehicle as shown in Fig. 8. A simulation of OP1 is carried out to determine the maximum thickness of the tiles and the number of tiles that could fit in the Cargo Vehicle. The final configuration of radial tiles was decided in collaboration with other Payload WP members. The maximum tile thickness was set to 20 cm, and the manoeuvre duration was set to 60 seconds to minimise potential damage caused by impact in case of a collision.

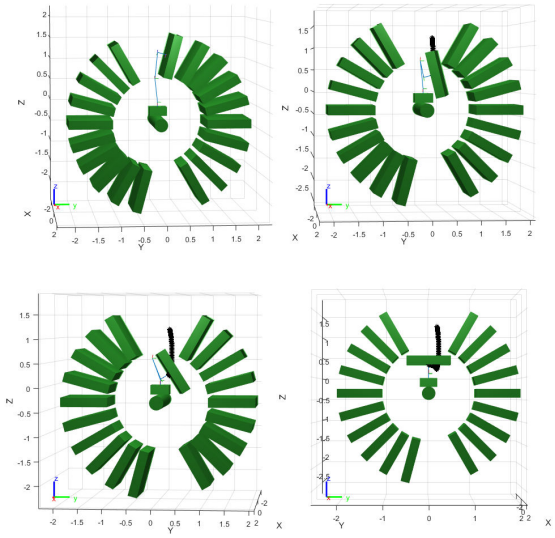

Fig. 8. Operation 1 (OP1) scenario simulation.

The second simulation scenario, OP2, considers the process of placing the first tile of the structure. As there was no structure for the robot to navigate over, the first tile had to be removed from the Hub and attached to the Hub's entrance. The main constraint for this manoeuvre was passing the tile through the Hub door (1.5 m x 1.6 m)

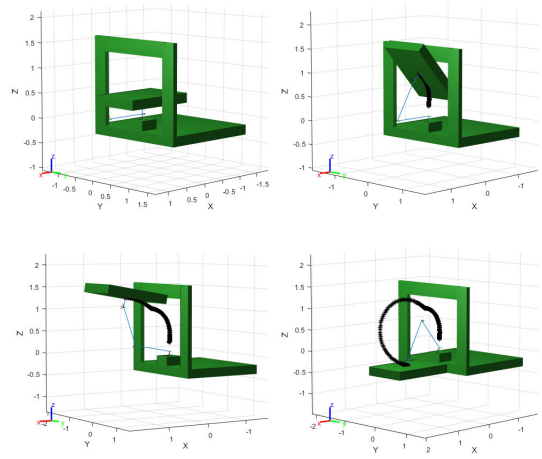

Fig. 9. Operation 2 (OP2) scenario simulation.

without collision. To achieve this, multiple trajectories are generated for the robotic arm carrying the tile through the door.

The duration of the manoeuvre for OP2 was set to 60 seconds, considering the slow and accurate motion execution to avoid the collision with the door frame.

In the third operation OP3, the tile is placed on the extended structure connecting with the existing tile. This operation considers the worst-case manoeuvre due to the higher disturbance torques and energy consumption. To fulfil the constraint of peak disturbance torques not exceeding 5 N·m in absolute value, the manoeuvre duration was selected accordingly. Multiple trajectories were generated, with durations ranging from 10 to 60 seconds, and tile masses between 30 and 60 kg. Eventually, a manoeuvre duration of 30 seconds and a maximum tile mass of 50 kg were chosen, resulting in a maximum disturbance torque of 4 N·m in absolute value, providing a 20% margin concerning the limit. This solution is simulated and shown in Fig. 9. The angular positions, velocities, accelerations, joint torques, joint mechanical power, disturbance torques, and energy consumption were all plotted and analysed in MATLAB.

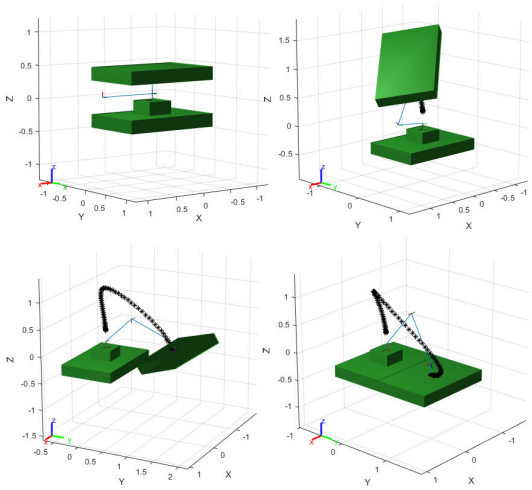

Fig. 10. Operation 3 (OP3) scenario simulation.

4.4 Path planning

A path planning approach is developed to move the assembler from a given position to a target assembly position. This approach considers the constraints on maximum torque controlled by AOCS and assembly time of six months maximum. The velocity and acceleration extrema of the assembler path are obtained to compute the power consumption for the robot locomotion that provide the expected assembly time of the structure. This approach begins with the creation of a grid that defines the overall dimensions of the structure, determining the number of tiles along each axis based on the mission. Then, a starting point shall be defined. Afterwards, A matrix is generated to encapsulate desired positions, each representing the centre of a tile. Distances from the starting position to these desired locations are calculated and integrated into the matrix, subsequently sorted by proximity to the Hub.

Analogously, a “direction of movement” matrix is defined, which indicates the direction to search for the neighbour tiles. Finally, initialisation of other inputs such as robot masses and tile properties are also required. Given the constraint that a robot can transport only one tile at a time, a loop is formulated within the main program. The algorithm systematically explores neighbouring positions to determine the most efficient route to the target, considering power requirements and turns.

The outcome of this program includes the total power consumption required of the assemblers and the total assembly time of the project. A flow chart for the approach is shown in Fig. 11.

The maximum and minimum accelerations of the assemblers are 0.0025 m/s^2 and 0.0015 m /s^2, respectively. The velocity calculated for the assembly process is 0.00279 m/s and 0.02 m/s to travel inside the vehicles. Consequently, the electrical power consumption of the locomotion is 2.9 W. Hence, the total assembly time is 148 days, 6 hours and 6 minutes, which is approximately 5 months, giving 1 month of margin from the time requirement. Finally, the maximum normal force that the linear actuator shall exert is 0.34 N to stop the assemblers.

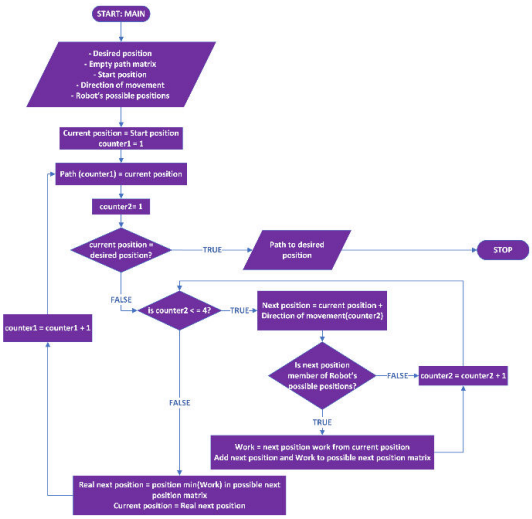

Fig. 11. Operation 3 (OP3) scenario simulation.

4.5 Design of the Supply Vehicle and Hub

In this section, the individual characteristics of the Supply vehicle and Hub are explored, along with the

internal subsystems within each structure, which formed separate work packages.

4.5.1 Supply vehicle

The supply vehicle serves its purpose as a cargo vehicle containing the tiles for the assembler to remove and assemble. In this subsection, the structure, configuration, power, communications and AOCS subsystems are detailed.

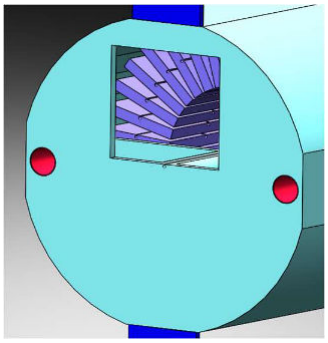

Fig. 13. Supply vehicle's back side.

4.5.1.1 Supply vehicle structure

Considering the highest possible payload capacity, the Supply Vehicle's fairing was designed as a cylinder of diameter 4.2 m and 12 m in length as shown in Fig. 14. This diameter is the largest possible with a Falcon Extended fairing while keeping a minimum of 10 cm clearance. (Falcon Extended fairing: 4.4 m diameter, 12.1 m straight height, 14.7 m height with a conical tapered top).

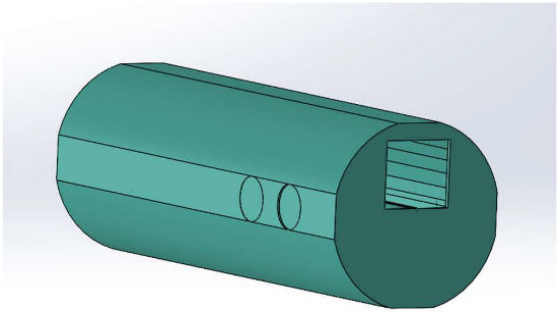

Fig. 14. Supply vehicle main structure.

The cylinder is not perfectly circular, and flat surfaces are necessary to provide 360° clearance for the thrusters. Also, the solar panels are stored inside the free volume created by these flattened surfaces and deployed afterwards. The main propulsion system is composed of two engines in the back, embedded, with two holes for the exhaust cones as represented in Fig. 13.

The SV's cylinder features a rail running through its centre that enables the assembler to access the payload

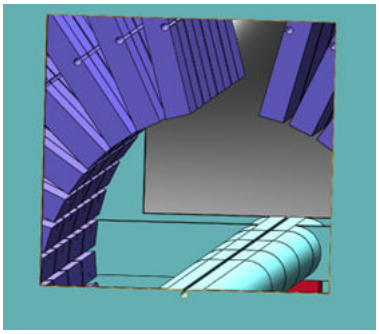

Fig. 12. Supply vehicle's rail system.

regardless of where it is stored. The proposed design offers a notable scalability advantage, allowing for the sequential docking of extra supply vehicles in a manner that aligns and connects their doors and rails. This arrangement enables the robotic assembler from the initial supply vehicle to conveniently access the payloads of the additional supply vehicles.

The rail is housed within an elliptical metal bar that spans the entire length of the SV as shown in Fig. 12. This bar has a flat surface on both the top and bottom, with four circular secondary rails intersecting the main rail to provide complete 360° access to the entire storage area.

4.5.1.2 Supply vehicle configuration

The internal volume of SV is composed of three parts: the propulsion system, the payload storage, and the subsystems compartment.

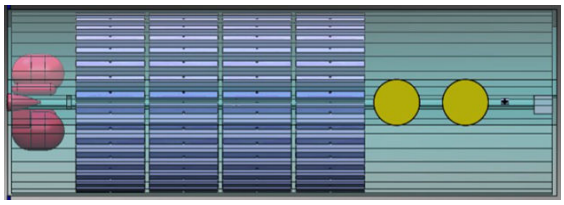

Fig. 15. Supply vehicle's configuration.

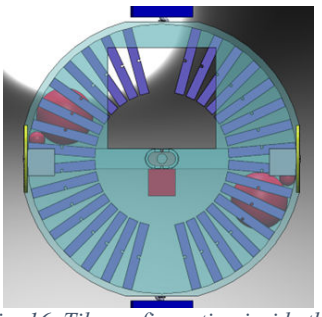

Fig. 16. Tile configuration inside the SV.

In Fig. 15, there are two propulsion systems shown in red. Each propulsion system contains a single propellant tank, a helium tank, and an engine. The purple rectangular shapes show the four rows of tiles stored in a

circular layout and the (right) empty section of the SV shows where the internal subsystems will be stored.

The selection of the tile configuration is based on the maximum number of tiles to be stored in a single launch and robustness to tile retrieval failure.

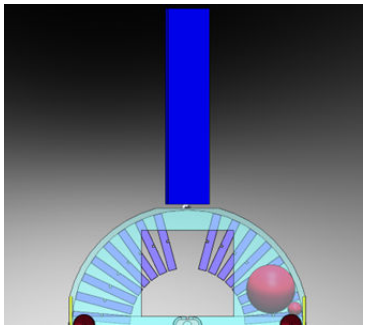

Fig. 17. Top SV's SP with the rotation and deployment system.

Assuming a payload thickness of 30 mm (simple solar panel example) and a minimum longitudinal clearance of 100 mm and a radial clearance of 30 mm, we used a radial configuration as shown in Fig. 16. It allows for 32 tiles to be arranged in a single row, with a total of four rows inside the SV. Therefore, this arrangement allows for a maximum of 128 tiles to be stored and then assembled.

The generous gap located at the top serves as the starting point for the assembly process, where the assembler initiates the task. Once the robot retrieves the first tile from the middle of its rail, it carries it through the supply vehicle and the Hub, and finally places it in its allocated position, thereby allowing the assembly of the next tile. However, this assumes that there are no tile jams or other hindrances during the operation.

To address this issue, a clearance is created in the base, and the orientation of the tiles is chosen to minimize losses. Assuming the assembler needs to start by assembling the tiles on the left section of the row represented in the Fig. 16, the robot can obtain eight tiles of the same orientation from the top and then acquire the last eight tiles from the bottom, repeating this process for the right side of the same row. Consequently, the maximum potential loss drops from 32 to 8 tiles in the event of a jam occurring in the very first tile of a section.

4.5.1.3 Supply vehicle power subsystem

Two rotary solar panels with panel dimensions 4.4 m x 1 m are proposed to power the SV systems.

The attachment between the solar panel and the SV is represented in Fig. 17 and it shows a simplified version of how the solar panels will attach to the SV whilst ensuring the solar panels remain sun pointing throughout its orbit. This identical system is mirrored on the underside of the SV. However, it should be noted that the location of the solar panels on the SV exterior is dependent on the mission application and the orbit, due to the consequences of shadowing.

4.5.1.4 Supply Vehicle communication subsystem

To ensure a 360° communication coverage, it was opted to employ two sets of two phased array antennas on two opposite sides of the vehicles as shown in Fig. 18 (yellow circles).

This technology provides a significant advantage over other antenna technologies as it can electronically alter the beam to transmit and receive data to relay satellites without requiring any mechanical or physical adjustments. This avoids the need for any movement or alignment of the antennas. The set of antennas is composed of one antenna of 1 m in diameter for telemetry tracking and command and one antenna of 1 m in diameter for payload data transmission.

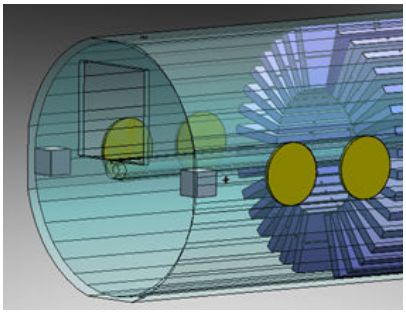

Fig. 18. Antennas configuration outside the SV.

4.5.1.5 Supply Vehicle Attitude Orbital Control Subsystem

The distinctive feature of the AOCS thrusters is that there are 32 thrusters arranged in 8 groups of 4 thrusters, each oriented 90° apart from the others.

This arrangement prevents them from being embedded in the same way as the antennas (side circular indentations) for exhaust clearance purposes.

4.5.2 Hub

The Hub serves its purpose as a central unit for the assemblers. In this subsection, the structure, power, communications and AOCS subsystems are detailed.

4.5.2.1 Hub main structure & configuration

The Hub carries the assemblers on rails. While in the launch phase, the assemblers are stowed on the secondary rail for safety. The main rail is reserved for the mission and the secondary rail is only utilised if one of the two robots malfunction. In such a scenario, the operational robot will tow the dysfunctional one to the secondary rail, ensuring that the primary rail remains clear for the rest of the mission.

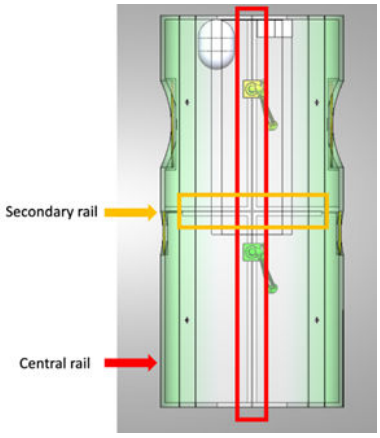

Fig. 19. Hub's internal configuration with rail intersection.

4.5.2.2 Hub power subsystem

In terms of power, the difference with the supply vehicle is the surface needed to meet the electrical requirements. As the supply vehicle, there are two solar panels (one at the top and one at the bottom) and each solar panel dimensions must be 5.1 m x 2.26 m.

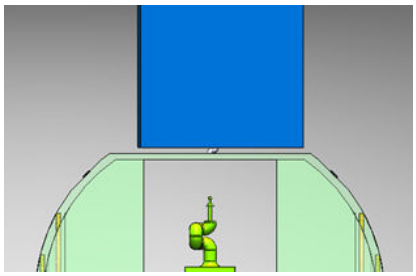

Fig. 20. Top Hub solar panel with rotation and deployment system.

Again, the attachment between the solar panel and the Hub represented in the Fig. 20 is a simplified concept of its functionality, demonstrating the solar panels' capacity to deploy and track the sun's movement. This identical system is mirrored on the underside.

4.5.2.3 Hub communication subsystem

To ensure a 360° communication coverage, it was opted to employ 2 sets of 2 phased array antennas on two opposite sides of the Hub as shown in Fig. 21 (yellow circles).

The set of antennas is composed of one antenna of 1 m in diameter for telemetry tracking and command and one antenna of 2 m diameter for payload data transmission.

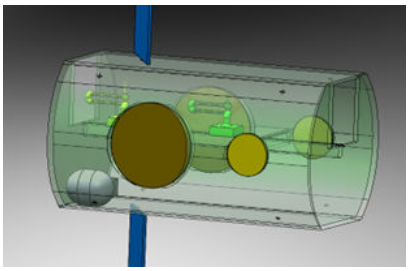

Fig. 21. Antennas configuration outside the Hub.

4.5.2.4 Hub Attitude, Orbital, Control Subsystem

This time, there are 16 AOCS thrusters arranged in 4 groups of 4 thrusters, each oriented 90° apart from the others. This arrangement prevents them from being embedded in the same way as the antennas (side circular indentations) for exhaust clearance purposes.

5. Mission Analysis

In this subsection, the mission analysis is reported to determine the ideal orbit type. Details on the propulsion and AOCS subsystems are then highlighted to ensure that this orbit is met for the mission.

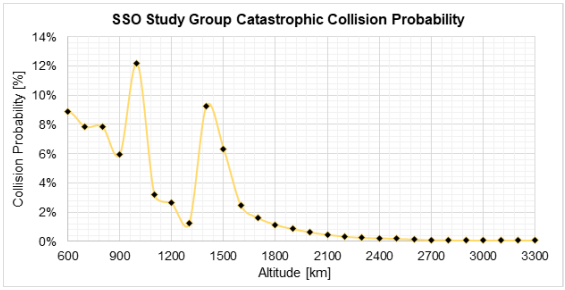

Fig. 22. Catastrophic Collision Probability Over 10 Year Mission Duration Disposal.

5.1 Orbit selection

A systems-based approach was utilised for the orbit selection process. The top three design drivers used for this analysis were catastrophic collision probability, eclipse fraction (for power generation) and atmospheric drag. Following on from the performance analysis, an evaluation of the orbit study groups concluded that a non-eclipsed, dusk-dawn 3300 km semi-major axis, circular SSO provided the best performance when comparing with the orbit selection design drivers. To compute the probability of a catastrophic collision between MARIO2 and orbital debris, an orbital collision risk assessment was conducted using ESA's MASTER [12] and DRAMA [13] software. Its results are plotted in Fig. 22.

It should be noted that an acceptable probability of a catastrophic collision was set to 0.1% over the mission lifetime and this requirement was achieved by the operational orbit selected for the mission.

A graveyard orbit is selected as a viable disposable method considering the space debris mitigation standards and guidelines and casualty associated with semi-controlled and uncontrolled re-entry of high mass systems as well as the unfeasible propellant consumption required to successfully perform a controlled re-entry.

5.2 Propulsion

The goals of the propulsion subsystem include defining requirements, design, and selection of propulsion subsystems for primary mission elements and spacecrafts (Hub & Supply Vehicle), utilising MATLAB software and STK12 for ΔV calculations and algorithm computation for the required manoeuvres. It also addresses the selection of launch vehicles, conducting two trade-studies to establish the requirements for the launcher to insert the spacecraft into desired mission orbit.

The Orbit Control Propulsion System consists of distinct propulsion systems tailored to each component of the mission. To begin with, The Hub's manoeuvring is performed by the use of monopropellant Hydrazine, specifically the Aerojet MR-106L [14]. This monopropellant is mainly used for pre-docked manoeuvres.

On the other hand, the SV implements a bipropellant approach, employing a combination of Monomethyl hydrazine (MMH) and Nitrogen Tetroxide (NTO) as propellants. The Ariane Group's 200N/10N bipropellant system [15] is chosen to meet the manoeuvring requirements. These bipropellant propellants are used for executing rendezvous and docking manoeuvres subsequent station-keeping.

With respect to the selection of launchers, the Hub's propulsion requirements are met by the Falcon 9 launcher [16], which features a re-usable 1st stage. In parallel, the Supply Vehicle's propulsion needs are met by the Falcon Heavy launcher as it is larger and carries more payload.

5.3 Attitude orbital control subsystem

The determination of the optimal orientation of the spacecraft is essential for the mission. In the case of large planar structures, the gravity gradient torque is the principal environmental torque that affects the structure over the others. In addition, the gravity gradient torque depends on the orientation. However, the selection of the orientation depends on the main attitude requirements and constraints that have the mission. In the case of MARIO2 mission, as it is a demonstration mission, there is no concrete constraints, and the orientation is decided to have the maximum stability possible. A stability study is carried out to determine the most stable orientation of the spacecraft. The result of this analysis concludes that the orientation that assures a stability on the three axis of the spacecraft is the one shown in the Fig. 23, which is just slightly more stable than main orientation shown in Fig. 3.

This orientation provides complete three axis stability; in the case of having a failure on the attitude actuation hardware, the orientation would remain stable, thus, providing constant sun pointing to the solar panels. However, as the tiles can require other orientation due to its specific requirements, the opted orientation for the mission is the main one shown in Fig. 3. The main reason was to validate the worst-case scenario configuration. With this orientation the gravity gradient torque is minimised, however, is unstable so an active control action would be required to keep the orientation of the spacecraft.

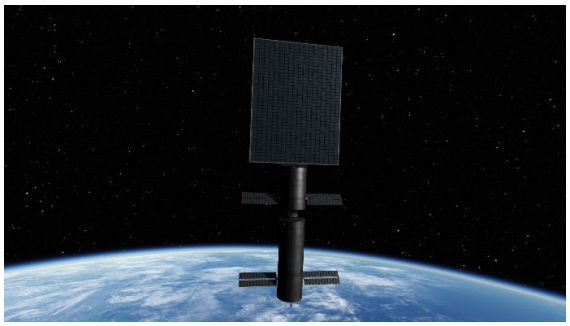

Fig. 23. Alternative orientation of the structure (for deep space observation).

To achieve the desired orientation and satisfy the attitude and orbital requirements, a moment gyros of 1.1 Nm maximum actuation torque is selected. In addition, seven sun sensors, four earth sensors, and two IMUs are selected as required sensor to satisfy the precision imposed by maximum deviation requirement.

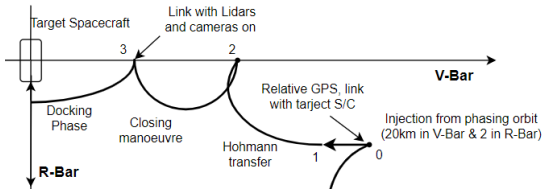

Fig. 24. R-bar proximity orientations and docking.

The R-bar approach [17, 18] is selected for the docking between the Hub and the supply vehicle. The proximity operations that end in the docking are described in Fig. 24, using relative navigation and Lidars as the main hardware. The spacecraft injected from the phasing orbit and starts an initial approximation via a Hohmann transfer into the target orbit. Then the spacecraft performs a closing manoeuvre and end the process introducing the chaser spacecraft in the R-Bar axis to perform the R-bar docking.

Upon thermally analysing the structures it was discovered that the mission application will dictate the Hub and supply vehicle orientation with respect to sun pointing, which will determine the solar panel location and orientation on the Hub and supply vehicle.

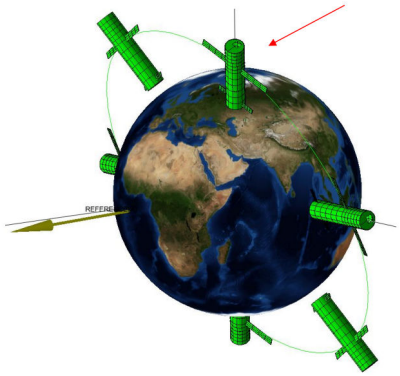

Fig. 25. Deep space observation orientation.

Deep space observation and sun facing observations require the Hub and supply vehicle to be oriented vertically and radially pointing outward from earth to ensure the tile structure is built such that the payload surface entirely faces either the sun (shown by the yellow arrow) or deep space, as shown in the Fig. 25. It can also be seen solar panels are located on the sides of the Hub and SV to ensure true sun pointing for the total mission duration.

The location of the solar panels with respect to the Hub and SV will change and be located on the tops and base of the Hub and the SV if the mission application changes that requires a partial sunlit payload tile, resulting in the following orbital configuration as seen in the Fig. 26.

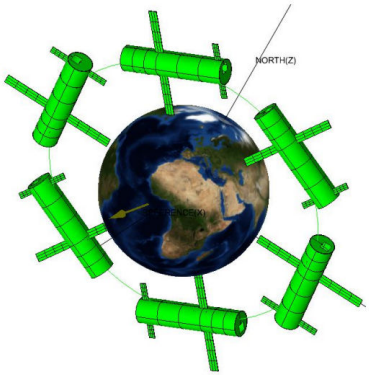

Fig. 26. Orientation with maximum solar efficiency in tiles (Sun perpendicular to the tiles).

6. Mechanical Design and Analysis

The structure for the in-orbit assembled large planar system consists of four mechanical sub-assemblies: tiles, Hub, SV, and robot assemblers. The current work encompasses the design and analysis for the structure and material selection for all the sub-assemblies.

6.1 Planar Tiles

Tiles are the basic building blocks of the planar structure. These parts act as the flatbed upon which the client's payload is laid. Thus, it becomes the elementary component between the space system and the client payload. Building a planar structure in space requires mechanical properties ensuring long-lasting structural support. Detailed trade studies and calculations were performed to obtain tile dimensions and shape. With the defined configurations, and based on requirements and constraints, the 2 primary sections of the tile structure: rail and sandwich panel were designed and evaluated for performance. The final tile design is shown on the left in Fig. 3. The designed specifications for the tiles are:

- 1 m x 1.5 m planar size.
- Height of the block tile: 110 mm.
- Selected bulk material: Carbon-Kevlar-Glass (CKG) fibre composite.
- Mass of about 20.5 kg per tile with 5% margin.

6.2 Hub and Supply Vehicle Outer casing

The design of the Hub and SV body casing also considered the internal components, configuration, and inputs from thermal analysis to evaluate the model and verify the compliance of set requirements. The casing geometries were defined as:

- Hub: 4.2 m diameter, 6.6 m height.
- SV: 4.2 m diameter, 12 m height.
- Casing Thickness: 20 mm (for both Hub and SV)
- Selected bulk material for the casing: Carbon-Kevlar-Glass (CKG) fibre composite.
- Shielding bumper layer: 5 mm Ti-Al-nylon layer.
- Shielding bumper spacing: 50 mm.

6.3 Interfaces and Mechanisms

A mechanical androgynous interface is proposed to interconnect tiles which is shown in Fig. 29. The benefit of this design is that interlocks two tiles with any orientation.

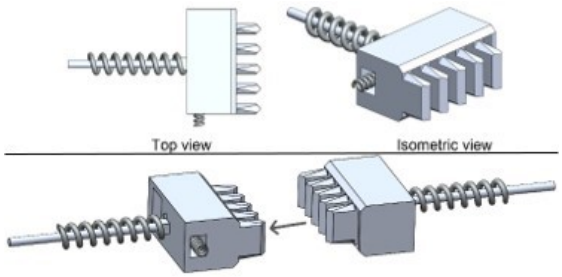

Fig. 29. Design of Tile-to-Tile interface with interlocking fingers adjustable by the small side spring and pushed into place by the large rear spring.

The interlocking mechanism adjustable with 2 springs in lateral and longitudinal directions of the interface makes it an ideal candidate as it satisfies the required degree of motion without any requirement for external power. Fatigue or impact related simulation are carried out to satisfy the requirements on performance and life.

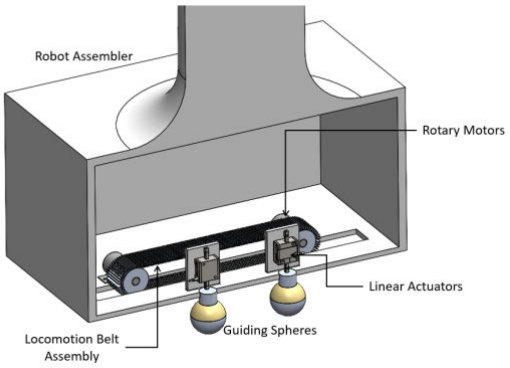

Fig. 28. Final design for Robot assembler locomotion mechanism.

The robot locomotion (see Fig. 28) encompasses the mechanism installed inside the robot assembler which provides the translation motion, along with the interface that keeps direct and continuous contact between the rails and the robot assembler. The proposed solution is a rail-based locomotion using negative slippage metal tractive belt-induced motion to move forwards and backwards.

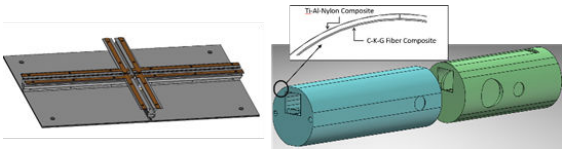

Fig. 27. Final design of Tiles (left) and final design of Hub and SV casing (right).

The mechanism uses guiding spheres to lock the robot with tile layout preventing it to flyout, provide electrical connection, and assist in breaking the robot locomotion.

The designed and developed concepts in the current work were evaluated based on their performance and assessed by implementing various analysis and simulations: structural, vibrational, thermal, multi-body, fatigue, and debris impact (see Fig. 31).

The impact testing analysis was performed for small and large sized debris pieces on the planar tiles, and as an induced load on the interlocking mechanism as well. The analysis performed have two different formats: single debris piece impact, and multiple debris piece impact

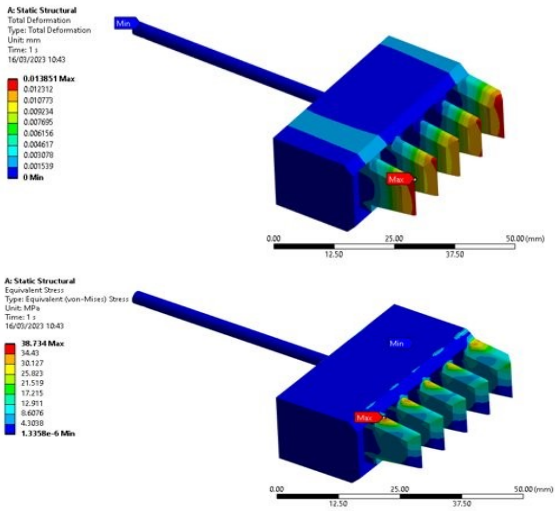

Fig. 31. Structural analysis of the mechanical interfaces for different cases of experiencing vibrational loads, thermal and radiation loads, impact loads, bending and torsion loads.

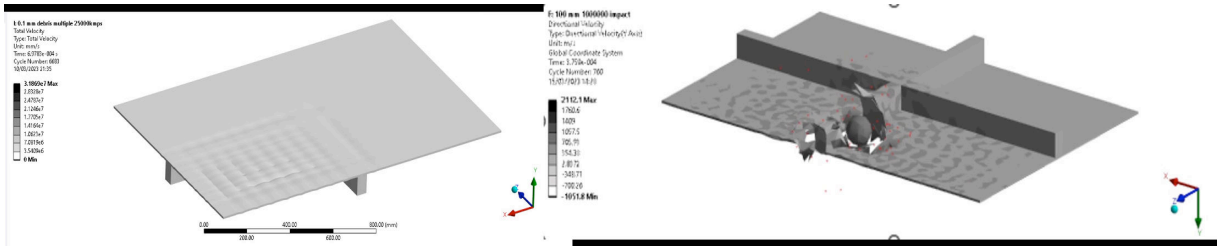

Fig. 30. Simulation results for Debris Impact testing: Multiple debris piece head-on impacts (left), Single debris piece inclined impact (right).

simultaneously, and with different angle of attack: head-on and inclined. The obtained results for small and large sized debris pieces at 2.5 km/s threshold velocity is shown in Fig. 30.

6.4 Thermal Analysis

The thermal analysis of multiple-armed robots for in-orbit operations conducted in ESATAN-TMS, successfully led to the selection of appropriate thermal protection for the Hub, Supply Vehicle, Robots and associated subsystems within the desired sun-synchronous orbit. The analysis was two-fold and considered the most extreme thermal environments of true sun-facing and deep-space facing payload applications within the selected structural configuration in orbit. A combination of gold interior and kapton exterior coatings for the Hub and supply vehicle were found to effectively radiate a portion of absorbed heat flux from the outer structure to the inner structure, where the gold interior would conduct this heat to the inner subsystems, reducing the need for active thermal control.

The bulk of the analysis involved determining operating temperatures of subsystem electrical components from manufacturing datasheets, applying margins and selecting coatings resulting in the closest margin operating temperatures to those experienced in orbit. Radiative analysis and hand calculations were performed to determine heat radiated from switched on components. The TCS selection process considered both worst-case cold (switched off components) and hot scenarios (switched on components) over an entire orbit.

For deep-space facing applications, specific subsystem coatings & active hardware included gold and heaters for the Hub's AOCS subsystems, black paint for communications & power subsystems, aluminium 6061-T6 for structures, white epoxy and a heater for data handling and kapton with a heater for propulsion, where heaters are to be 100W flexible polyimide kapton heaters. In sun-facing applications, the same coatings are to be applied to the AOCS, communications and propulsion subsystems, but different coatings were required for structures (gold) and data handling (kapton). The supply vehicle requires kapton, black paint, white epoxy aluminium 6061-T6 and kapton coatings for the AOCS, communications, data handling, structures, power and propulsion subsystems respectively in deep-space applications without any need for heaters. For sun-facing applications, the same coatings are required except for structures (kapton) and power (black paint).

The robots were designed to have bi-metallic spring actuated louvres all around the robotic base. This solution was selected as no single coating was adequate as a large amount of active control would be required along with a high radiating ability in each application which was considered not efficient. The bi-metallic spring actuated louvre offers a purely passive means of thermal control. The selected coatings and resulting temperatures for the robot subsystems in both the louvre open and closed positions are shown in Table 2.

Table 2. Robot subsystem temperatures resulting from coating selection with the louvre in the extreme (90 degrees) open and extreme closed position for both thermally extreme pointing applications.

Bi-metallic Spring Actuated Louvre System Temperatures (open) to (closed): Deep Space Applications				
Subsystem	Coating	Temp (°C)	Required Temperatures (°C) (with margins)	Active Control
Electrical	Kapton	18 ~ 21	0 (10) ~ (55) 65	N/A
Power	Kapton	5 ~ 31	0 (10) ~ (30) 40	N/A
Comms	Black Paint	-10 ~ 17	-20 (-10) ~ (50) 60	N/A
Arm	Black Paint	-9 ~ 63	0 (10) ~ (50) 60	Heater / Phase change material
Bi-metallic Spring Actuated Louvre System Temperatures (open) to (closed): True Sun Applications				
Electrical	Kapton	-51 ~ 11	0 (10) ~ (55) 65	Heaters
Power	Kapton	-50 ~ 36	0 (10) ~ (30) 40	Heaters
Comms	Kapton	-46 ~ 10	-20 (-10) ~ (50) 60	Heaters
Arm	Kapton	-90 ~ 42	0 (10) ~ (50) 60	Heaters

In addition, the selected materials and joining mechanisms were designed to account for thermal contraction and expansion over time in the interfaces of the assembled tile structures and Hub-supply vehicle. This analysis has been crucial in the development of multiple-armed robots for in-orbit operations enabling the selection of appropriate thermal control system design for each structure and its subsystems.

7. Electrical power subsystem

To provide power to multiple-armed robots for in-orbit systems (Hub, SV, and Assemblers), a space environment analysis, mechanical and power interface selection were conducted. This also included a power loss simulation analysis and solar and battery sizing.

The total power required from batteries according to power modes is 1931 W-Hr for the Hub and 1311 W-Hr for the SV (see Section 6. Budgets). Today's most efficient battery for aerospace applications is Lithium-Ion. With a 96% discharge efficiency and a specific energy >130 W-Hr, this type of battery was chosen. To size the solar arrays, many were discussed including mass, efficiency and resulting total area, the most efficient one was selected due to the Hub and SV solar array size limit. The Spectrolab XTE-SF (triple junction)

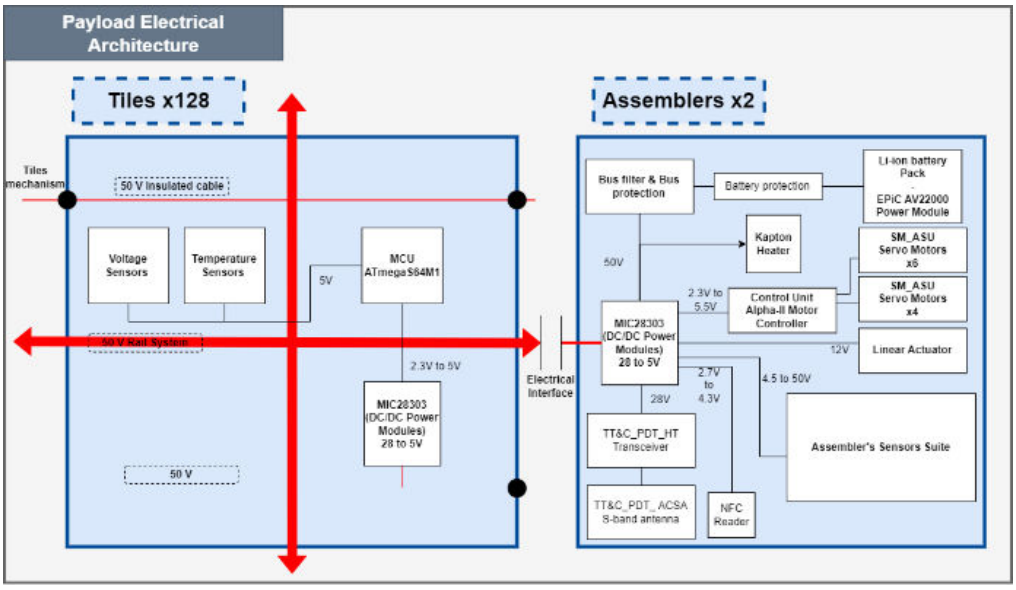

Fig. 32. Payload Electrical Architecture.

of 32.20% efficiency and a 10 years EOL array specific power of 243.71 W for a 11.6 m^2 panels of the Hub and 4.4 m^2 panels for the SV. The electrical properties of Spectrolab cells were discussed to size the panels accurately for all systems and solar panels materials were also studied, they are made of Aluminum Honeycomb, thin Kevlar fibers, cover glass, Spectrolab cells and joints/connectors.

The design of the rail was impacted by space harsh environment for electrical components, extreme temperatures, charging effects, surrounding plasma, atomic oxygen as well as radiation effects. As our mission is to operate in a sun-synchronous orbit at ~3000 km altitude, one major factor is ionospheric plasma due to solar UV that ionizes oxygen and nitrogen atoms in LEO. A high concentration of free electrons implies avoiding exposed conductors with potentials superior to 100 V within the magnetosphere. The decision of a 50 V Rail System was made to avoid plasma dangerous effects and power losses considerations. Fig. 32 highlights the electrical architecture of the tile structure and the assemblers powered through a 50V rail system.

8. On-Board Data Handling and Autonomy

The use of an Autonomy Requirements Engineering (ARE) methodology [19] in the design and development of MARIO2 has proven to be effective in ensuring that the autonomous systems meet the desired operational goals and objectives. By eliciting, analysing, specifying, validating, and managing autonomy-related requirements throughout the system development life cycle, we have been able to design a space mission that operates autonomously in a safe, reliable, and efficient manner.

The ARE approach identifies and manages risks associated with autonomy, such as potential failures or unexpected behaviour, resulting in the design of an appropriate Software Operation Modes for each system as shown in Fig. 33 for the Hub.

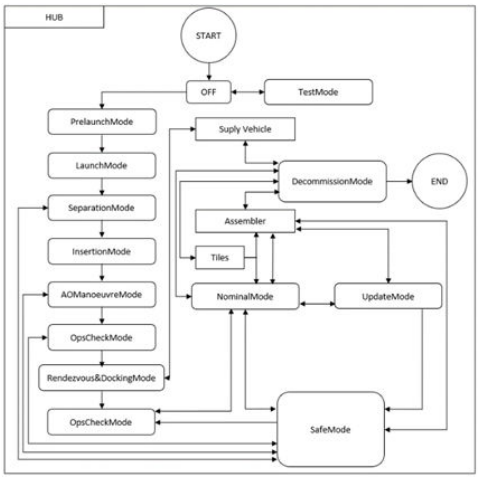

Fig. 33. Software operation modes.

8.1 Communication subsystem

The communication Subsystem is responsible for transmitting housekeeping data and other mission-related data from components like SV, Hub, Assemblers, and Tiles to the ground. It also receives telecommands, control data, and Position, Navigation, and Timing data.

For the Communication subsystem, requirements were established, and discussions with electrical and payload subsystems helped identify constraints and design drivers. A conceptual communication architecture was developed (see Fig. 34), considering data types and traffic direction. An analysis of the operational orbit highlighted communication challenges, leading to the

exploration of alternative solutions. Relay communication was selected, and the space relay and ground segment networks were chosen based on services provided by reputable space agencies such as NASA and ESA. Detailed analysis, including simulation, helped determine the network topology and characteristics of antennas. Link budgets were defined, and redundancy measures were incorporated into the communication subsystem design. Suitable communication hardware was selected based on factors like weight, power, and performance.

The communication topology is shown in Fig. 34. where all the communication nodes are depicted as well as the type of communication.

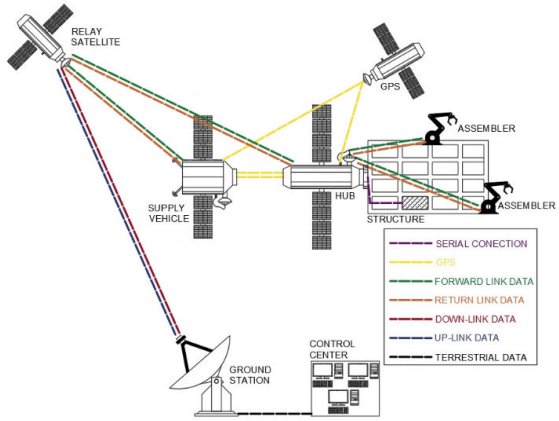

Fig. 34. Design of Tile-to-Tile Interface with interlocking fingers adjustable by the small side spring, and pushed into place by the large rear spring.

Among the communication nodes, the control centre assumes has the central role of overseeing and managing the telecommunication systems, monitoring network traffic, and ensuring the data is link is always on and bidirectional. The ground stations serve as terrestrial facility that consists of several antennas that enables the transmission of uplink TT&C data to relay satellites and receiving downlink TT&C and payload data, thus establishing the link between the spacecraft and ground control centre. Then, the Relay Satellites are positioned as intermediaries to amplify and relay signals between Ground Stations and the SV and Hub.

In addition to relay satellites, GPS Satellites in MEO orbit will precise positioning and synchronization. The Supply Vehicle undertakes several communication tasks, including data exchange with relay satellites, reception of absolute GPS data from GPS Satellites, and interaction with the Hub for relative GPS data transmission. At the same time, the Hub, acts as a central director that facilitates a forward Link TT&C data reception from relay satellites and a return Link TT&C and payload data transmission. Besides, it also manages the assemblers by overseeing the assembly process.

The assemblers are constantly receiving a forward link TT&C data from the Hub and simultaneously transmitting a return link TT&C and payload data. Finally, the Tiles participate in the communication network by transmitting wired TT&C data to the Hub and employing NFC technology for communication with Assemblers to accurately indicate the tile at which the assembler is at.

This communication subsystem integrates diverse nodes with distinct roles enables real-time data exchange, synchronization, and coordination providing a solid base for the mission in-orbit assembly.

9. Budgets

The overall budgets for each element are shown in Table 3. The mass budget was constrained by the amount of payload mass the Falcon 9 and Heavy were able to carry into orbit. An appropriate mass margin was given to each subsystem according to ESA's margins philosophies [20].

Table 3. Overall MARIO2's system budgets

	Mass [Kg]	Power [W]	Data [kbps]	ΔV [m/s]	Cost [M $]
Hub	5869	1567	6.19	17	91.99
Supply Vehicle	8853	1324	17044	217	136.64
1 Tile	21	2	3.22	-	0.17
1 Assembler	52	597	15080	-	14.26
Total Mission	17976	4241	47624	234	439.67

Each The table encompasses five columns, each representing a different parameter including mass, power requirements, data transmission rates, delta V and cost in millions of dollars. row corresponds to a different element of the mission and six rows, with each row corresponding to a specific mission component.

The Hub´s mass distribution is depicted in Fig. 35 where the structure and the AOCS subsystem combined takes around 90% of the total mass as this will be the central node which will take care of station keeping of the entire structure as well as coordinating the assembler´s tasks.

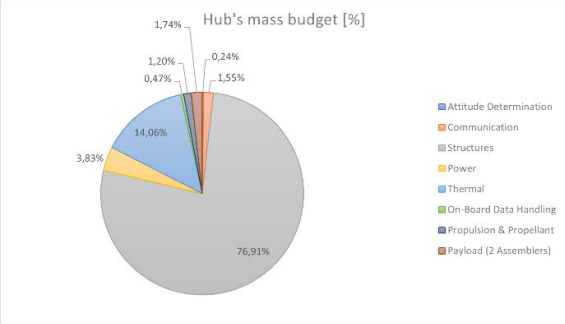

Fig. 35. Hub's mass budget breakdown.

A similar distribution is also present in the supply vehicle. The principal objective is to maximize the number of tiles, i.e., payload, to be transported. Using the circular distribution of tiles, this configuration enables for 128 tiles which is around 26% of the vehicle's total mass as shown in Fig. 36.

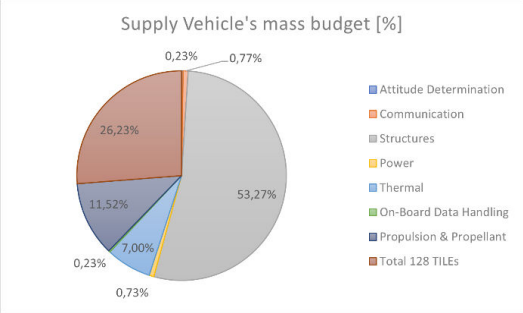

Fig. 36. Supply Vehicle's mass budget.

Analogously, the assembler's mass distribution is almost identical (see Fig. 37). All the instruments are concentrated in its base and more than 60% of the mass comes from the structure.

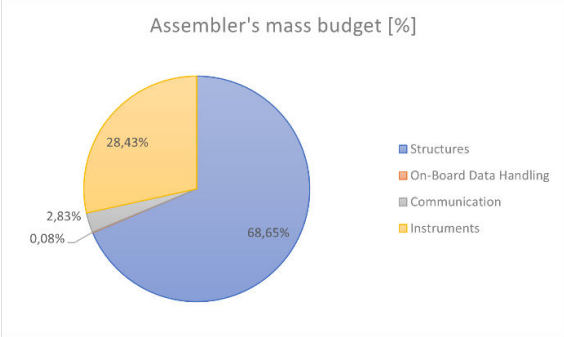

Fig. 37. Assembler's mass budget breakdown.

10. Conclusions

This paper details a conceptual design for an In-Orbit Robotic Assembly demonstration mission. The aim is to describe and conceptually develop the novel technology as well as the systems necessary of a robotic assembly mission for large space structures. The work developed serves as a reference source or baseline for sustainable future space developments in assembling large space structures, through the standardisation, repurposability and scalability of its elements and technologies.

The Multiple Arm Robot for In-Orbit Operations mission concept consists of a robotic arm assembler on rails, an array of modular payload tiles, a systems Hub spacecraft, and a cargo supply vehicle spacecraft. The assembler is capable of traversing between the Hub and Supply Vehicle with the tiles and assemble them outside the spacecraft to form the large space structure. The assembler's design and movement algorithm were optimised in order to maximize the assembly performance of its operations without causing unnecessary disturbances. The rail locomotion was utilized in order to give power, data and structural integrity to the assembled structure whilst providing mobility to the assembler. The tile is designed to act on an individual system level, having access to power and data from the spacecraft, and allowing for it and the payload to be independently removed or inserted from the structure. The Hub spacecraft is the main source of power, communications, computing and AOCS for the structure and assemblers during assembly operations. The supply vehicle holds the tile and payload cargo necessary to be assembled during the mission and acts as the point of storage for the material at either end of life or when out of commission. Both the Hub and SV are designed to be stackable, to allow for the scaling of the mission and structure size or capability by introducing additional material and system control.

The orbit selected for this mission was a Sun Synchronous orbit at 3300 km of altitude, allowing for a constant illumination for the power system of the spacecraft. The spacecraft, tile and assembler's power, communication, structural and thermal subsystems were sized and optimised for the orbital conditions. The mission aims to demonstrate the assembly capabilities for a large space structure utilizing robotic assemblers over the course of two years. After the commissioning phase the technologies would be stowed away inside the spacecraft and deposited into a graveyard orbit for decommissioning, reuse, or repurposing.

Through this paper the mission concept, and its budgets alongside the different necessary systems and subsystems in the architecture are discussed. The demonstration technology is designed to enable more efficient and effective space structure assembly missions by creating a standardised reference starting point and delving into scalability considerations. Ultimately, this research contributes to the development of advanced robotic systems for space exploration and infrastructure deployment.

Acknowledgements

The MARIO2 project was carried out as a group design project as part of the authors' MSc course in Astronautics and Space Engineering at Cranfield University, UK. The authors would like to acknowledge the excellent support of our supervisor Dr Leonard Felicetti and Dr Saurabh Upadhyay, who guided us throughout the project and assisted with the writing of this paper. The authors would also like to thank the MSc teaching staff for their support during the course. The presenting authors also would like to extend their heartfelt appreciation to Cranfield University, AIRBUS and GMV for their generous sponsorship, which made it

possible for them to attend and present the research results in Baku, Azerbaijan 2023.

References

[1] Flores-Abad, A., Ma, O., Pham, K., & Ulrich, S. (2014). A review of space robotics technologies for on-orbit servicing. Progress in Aerospace Sciences, 68, 1–26. https://doi.org/10.1016/J.PAEROSCI.2014.03.002

[2] Underwood, C., Pellegrino, S., Lappas, V. J., Bridges, C. P., & Baker, J. (2015). Using CubeSat/micro-satellite technology to demonstrate the Autonomous Assembly of a Reconfigurable Space Telescope (AAReST). Acta Astronautica, 114, 112–122. https://doi.org/10.1016/J.ACTAASTRO.2015.04.008

[3] Jamie Carter. (2022). The Webb Space Telescope Is Fully Deployed And 'Could Now Last 20 Years' Says NASA But What Happens Next? Retrieved April 16, 2023, from https://www.forbes.com/sites/jamiecartereurope/2022/01/10/the-webb-space-telescope-is-fully-deployed-and-could-now-last-20-years-says-nasa-but-what-happens-next/?sh=2bd622e04e95 , (accessed 25.06.23)

[4] Deremetz, M., Debroise, M., De Stefano, M., Mishra, H., Brunner, B., Grunwald, G., Roa, M. A., Reiner, M., Z´avodn´ık, M., Komarek, M., D'Amico, J., Cavenago, F., Gancet, J., Govindaraj, S., Letier, P., Ilzkovitz, M., Gerdes, L., & Zwick, M. (2022). Design and integration of a multi-arm installation robot demonstrator for orbital large assembly.

[5] European Space Agency. (2023). Space Debris User Portal. Retrieved April 16, 2023, from https://sdup.esoc.esa.int/ , (accessed 25.06.23)

[6] NASA. (2023a). Restore-L: Proving Satellite Servicing. Retrieved April 19, 2023, from https://www.nasa.gov/sites/default/files/atoms/files/restore_1_factsheet_092717.pdf (accessed 25.06.23)

[7] Li, W. J., Cheng, D. Y., Liu, X. G., Wang, Y. B., Shi, W. H., Tang, Z. X., Gao, F., Zeng, F. M., Chai, H. Y., Luo, W. B., Cong, Q., & Gao, Z. L. (2019). On-orbit service (OOS) of spacecraft: A review of engineering developments. Progress in Aerospace Sciences, 108, 32–120. https://doi.org/10.1016/J.PAEROSCI.2019.01.004

[8] Li, D., Zhong, L., Zhu, W., Xu, Z., Tang, Q., & Zhan, W. (2022). A Survey of Space Robotic Technologies for On-Orbit Assembly. Space: Science & Technology, 2022. https://doi.org/10.34133/2022/9849170

[9] XUE, Z., LIU, J., WU, C., & TONG, Y. (2021). Review of in-space assembly technologies. Chinese Journal of Aeronautics, 34 (11), 21–47. https://doi.org/10.1016/J.CJA.2020.09.043

[10] Miller, David W., Swati Mohan, and Jason Budinoff. "Assembly of a Large Modular Optical Telescope (ALMOST)." Space Telescopes and Instrumentation 2008: Optical, Infrared, and Millimeter. Ed. Jacobus M. Oschmann et al. Marseille, France: SPIE, 2008. 70102H-11. 2008 SPIE--The International Society for Optical Engineering.

[11] Deremetz, Mathieu & Debroise, Maxence & De Stefano, Marco & Mishra, Hrishik & Brunner, Bernhard & Grunwald, Gerhard & Roa, Maximo A. & Reiner, Matthias & Zåvodnik, Martin & Komarek, Martin & D'Amico, Jurij & Cavenago, Francesco & Gancet, Jeremi & Govindaraj, Shashank & Letier, Pierre & llzkovitz, Michel & Gerdes, Levin & Zwick, Martin. (2022). Design and Integration of a Multi-Arm Installation Robot Demonstrator for Orbital Large Assembly.

[12] The European Space Agency. MASTER (8.0.3) [Software]. 2022. Available at: https://sdup.esoc.esa.int/ (accessed: 01/02/2023).

[13] The European Space Agency. DRAMA (3.1.0) [Software]. 2019. Available at: https://sdup.esoc.esa.int/ (accessed: 01/03/2023).

[14] Aerojet Rocketdyne. (n.d.). In-Space Data Sheets. Available at: https://www.rocket.com/sites/default/files/documents/In-Space%20Data%20Sheets%204.8.20.pdf (accessed: 01/03/2023).

[15] ArianeGroup. (n.d.). Hydrazine Thrusters. Available at: https://www.space-propulsion.com/spacecraft-propulsion/hydrazine-thrusters/index.html (accessed: 01/03/2023).

[16] SpaceX. (2021, September). Falcon User's Guide. Available at: https://www.spacex.com/media/falcon-users-guide-2021-09.pdf (accessed: 01/03/2023).

[17] Wigbert Fehse. 2009. Automated Rendezvous and Docking of Spacecraft. Cambridge University Press.

[18] MCB, NASA, HEOMD. 2019. International Rendezvous System Interoperability Standards (IRSIS).

[19] Vassev, E. (2013). Autonomy Requirements Engineering. Available at: https://indico.esa.int/event/42/contributions/2442/attachments/1964/2273/Autonomy_Requirements_Engineering.pdf (accessed: 01/03/2023).

[20] European Space Agency. (2012). Margin philosophy for science assessment studies. Available at: https://sci.esa.int/documents/34375/36249/1567260131067-Margin_philosophy_for_science_assessment_studies_1.3.pdf (accessed: 01/03/2023).

In-orbit assembly: a baseline for large space structures through standardised tiles and interfaceable elements

Ji Zhang, Yi Qiang

2023-07-04

Ji Zhang YQ, Alão S, Fernandes JN, et al., (2023) In-orbit assembly: a baseline for large space structures through standardised tiles and interfaceable elements. In: 74th International Astronautical Congress (IAC), 2-6 October 2023, Baku, Azerbaijan.
https://dl.iafastro.directory/event/IAC-2023/paper/78354/